PCCP

PAPER

View Article Online
View Journal | View Issue

Cite this: *Phys. Chem. Chem. Phys.*, 2024, **26**, 24455

Shape and interactions of the synthetic repellent DEET†

Otger Crehuet,[ab] Andrea Vázquez,[ab] Pablo Pinacho,[ab] Aran Insausti,[ab] Elena R. Alonso,‡[ab] Francisco J. Basterretxea[a] and Emilio J. Cocinero*[ab]

Received 6th June 2024,
Accepted 11th August 2024

DOI: 10.1039/d4cp02315c

rsc.li/pccp

N,N-Diethyl-3-methylbenzamide (DEET) is the most widely used insect repellent, exhibiting high efficiency against a wide variety of species. In this work, a comprehensive isolated-molecule investigation of DEET was conducted using chirp-excitation Fourier transform microwave (CP-FTMW) spectroscopy within the frequency range of 7–14 GHz. Four out of the eight theoretically predicted conformers were detected and grouped in pairs based on their rotational constants and planar moments of inertia. We also studied the non-covalent interactions of DEET by characterizing the attractive and repulsive forces, which could explain the energetic ordering of the four conformers. In addition, DEET has a methyl top bound to the benzyl ring which is predicted to rotate almost freely with respect to the molecular framework.

Introduction

The use of insect repellents is one of the most common ways to prevent the spread of diseases transmitted by disease vector insects. For that purpose, plant-based compounds have been used for thousands of years with satisfactory results. However, in the mid-20th century, several synthetic repellents were developed that were more effective, longer lasting, and less noticeable than their natural counterparts.[1] Some of these synthetic repellents are designed for specific insects, although there are repellents that work against a wide variety of species.[2] By far the most widely used synthetic repellent is *N,N*-diethyl-3-methylbenzamide ($C_{12}H_{17}NO$), also known as DEET (Fig. 1).[3]

DEET is a yellowish oil that can be applied to clothing or directly to the skin to protect against mosquitoes, fleas, ticks, and many other insects. It is the most effective and widely used compound in commercial repellents.[3] However, after more than five decades of use, its mechanism of action is still not well understood.[4] Some studies suggest that DEET interferes with the mosquito's olfactory receptors involved in detecting 1-octen-3-ol,[5] or reduces the sensitivity of detecting lactic acid,[6] both components of human sweat. The existence of a specific DEET-sensitive olfactory receptor has also been suggested.[7]

An understanding of the possible spatial arrangements of DEET is necessary because the molecule's structure, key functional groups, and intramolecular forces all play a role in its behaviour and effectiveness. By understanding its conformational panorama, we can better comprehend its interactions within complex environments, such as solvation or protein binding. A useful strategy is to study the molecule in an isolated medium to obtain its intrinsic properties. Gas-phase investigations are a powerful approach that allows for isolated-molecule studies, avoiding interference from the medium, such as solvents or crystals.

In this context, rotational spectroscopy is a unique technique[8] because of its unsurpased resolution, capable of discriminating unambiguously between tautomers,[9] conformers,[10] isotopologues[11] and enantiomers.[12,13] Due to the significant advances made in this field in the last decade, chirp-excitation Fourier transform microwave (CP-FTMW) instruments allow the acquisition of broadband rotational spectra (several GHz) in a single frequency step, which in practice means shorter measurement times compared to a stepped

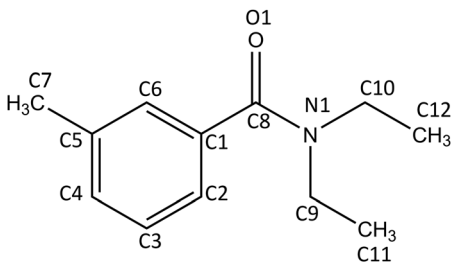

Fig. 1 Chemical formula of *N,N*-diethyl-3-methylbenzamide (DEET) and atom labelling.

[a] *Departamento de Química Física, Facultad de Ciencia y Tecnología, Universidad del País Vasco (UPV/EHU), Leioa, 48940, Spain. E-mail: emiliojose.cocinero@ehu.es; Web: https://grupodeespectroscopia.es/MW/*
[b] *Instituto Biofisika (CSIC, UPV/EHU), Leioa, 48940, Spain*

† Electronic supplementary information (ESI) available. See DOI: https://doi.org/10.1039/d3cp05104h

‡ Current address: Grupo de Espectroscopía Molecular, Edificio Quifima, Parque Científico UVa, Universidad de Valladolid, Valladolid, 47005 Spain.

survey scan that has to average many sections sequentially. Additionally, the spectrometer at the Universidad del País Vasco[14,15] has a sample injection, based in a pulsed valve system, that allows it to work with three nozzles simultaneously, improving the integration time needed to achieve the desired signal-to-noise ratio by an order of magnitude, while decreasing the sample consumption.

This study presents the use of a CP-FTMW spectrometer coupled to supersonic expansion along with molecular mechanics and DFT calculations to explore the potential energy surface of DEET, characterize its dominant conformations and study the intramolecular interactions that stabilize them. The aim is to facilitate future studies on DEET's interactions with biological receptors and to understand its mechanism of action.

Methodology

Computational modelling

A multi-step strategy was employed, which has successfully worked in several reported systems.[16,17] First, an exhaustive conformational search was performed on DEET using a fast molecular mechanics method to find stable geometries. The Macromodel software[18] was used to implement advanced Monte Carlo and large-scale low mode conformational search algorithms. The Merck molecular force field (MMFFs)[19] was selected, which has been parametrized for a wide variety of organic functional groups, including amides, and provides good results for conformational searches. In the present case, not all the possible conformers were found by this method (see below). The missing structures were drawn using chemical intuition. The resulting structures were reoptimized using density functional theory (DFT) calculations with the B3LYP[20,21] functional and the def2-TZVP basis set. Grimme's dispersion correction and Becke-Johnson damping were also implemented.[22] The computations included harmonic frequencies to confirm the geometries of the minima and obtain their zero-point corrected energies. The calculations were conducted using Gaussian16 and Orca 5.0.[23,24] Fig. 2 and Table S1 (ESI†) show the structures and present the rotational parameters and energies for all the conformers. Table 1 presents the rotational parameters and energies obtained by DFT compared to the experimentally obtained results for the observed conformers.

Experimental details

The CP-FTMW spectrometer at the Universidad del País Vasco was used to record the rotational spectrum.[14] The instrument is based on Pate's original design[25] and has been previously described.[15] To bring the DEET sample to the gas phase, it was heated to 423 K. The resulting vapours were diluted in Ne as a carrier gas at 2 bar and then expanded adiabatically through a small orifice into a vacuum chamber as pulses of 900 μs duration from a solenoid valve operated at a rate of 1 Hz. A 4 μs microwave chirp spanning a frequency of 7 GHz causes a macroscopic polarization of the sample. Following the excitation, a brief delay was allowed before recording 20 μs of the free induction decay (FID) signal. Ten excitation-detection cycles were collected on each supersonic expansion, resulting in an effective repetition rate of 10 Hz. The final spectrum was generated by FFT after co-adding 450 000 FIDs.

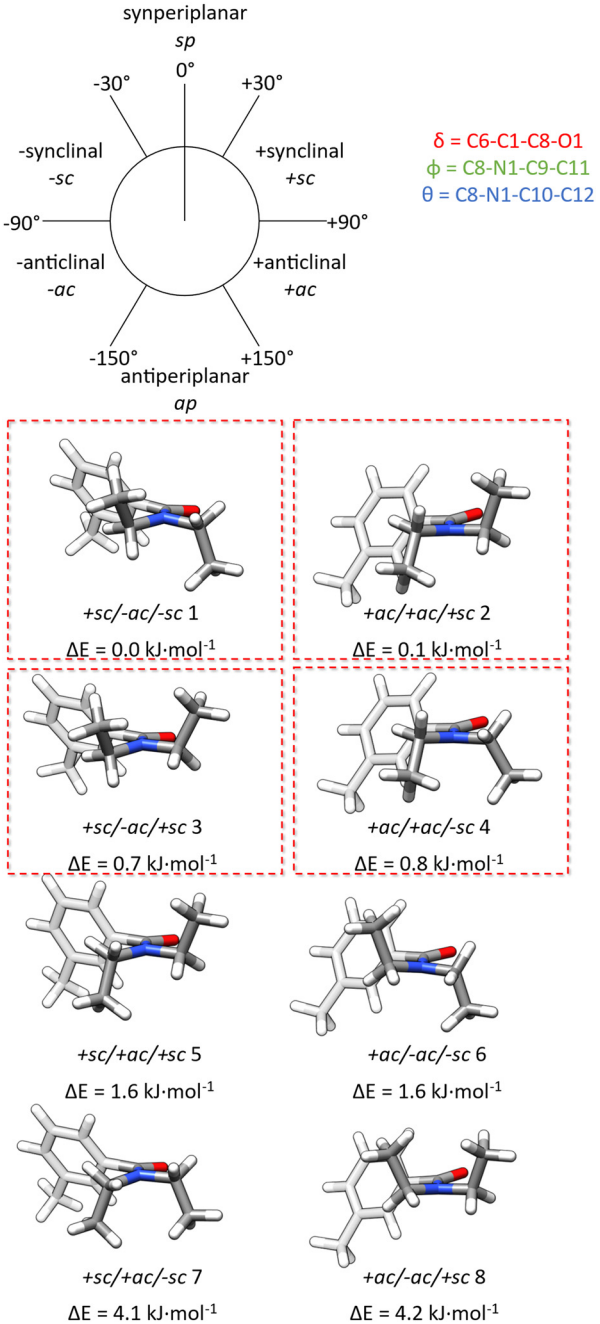

Fig. 2 Side view of the DEET conformers illustrating the nomenclature system. The conformers are grouped in almost isoenergetic pairs. The toluene group has been kept semi-transparent for better visualization. The conformers observed in this work are highlighted inside a red square.

Results and discussion

DEET potential energy surface

DEET has some flexibility arising from the relative orientation of its functional groups. The quantum chemical computations,

Table 1 Experimental rotational parameters and planar moments of inertia of the observed DEET conformers

	+*sc*/−*ac*/−*sc* 1		+*ac*/+*ac*/+*sc* 2		+*sc*/−*ac*/+*sc* 3		+*ac*/+*ac*/−*sc* 4	
	B3LYP	Exp	B3LYP	Exp	B3LYP	Exp	B3LYP	Exp
A [MHz][a]	1201	1198.98867(52)[i]	1178	1171.90097(88)	1313	1307.43287(61)	1134	1127.97608(24)
B [MHz]	415	415.63799(25)	436	437.10997(42)	399	397.92645(26)	440	439.35651(26)
C [MHz]	348	346.75536(23)	356	354.91352(51)	346	344.93085(30)	368	365.79335(29)
D_J [kHz][b]	0.018	0.01390(76)	0.013	0.0123(15)	0.01	0.01340(89)	0.016	0.01935(91)
D_{JK} [kHz]	0.167	0.0673(40)	0.084	0.119(12)	0.154	0.0650(84)	0.027	—
D_K [kHz]	0.015	0.1938(87)	0.031	−0.189(32)	0.026	—	0.112	—
χ_{aa} [MHz][c]	2.1	2.031(20)	1.7	1.558(38)	1.9	1.838(33)	2.1	1.959(34)
χ_{bb} [MHz]	−0.6	−0.685(19)	−0.3	−0.209(33)	0.6	0.636(29)	−0.2	−0.162(31)
χ_{cc} [MHz]	−1.4	−1.346(19)	−1.4	−1.348(33)	−2.5	−2.474(29)	−1.9	−1.796(31)
P_{aa} [μÅ^2][d]	1124	1125.92912(61)	1074	1074.44263(118)	1171	1174.32428(77)	1038	1041.91369(65)
P_{bb} [μÅ^2]	327	331.52205(61)	344	349.50708(118)	289	290.83607(77)	335	339.68333(65)
P_{cc} [μÅ^2]	93	89.98236(61)	84	81.74011(118)	95	95.70692(77)	110	108.35720(65)
$\lvert\mu_a\rvert/\lvert\mu_b\rvert/\lvert\mu_c\rvert$ [D][e]	≈0.0/2.7/2.3	No/Yes/Yes	0.6/3.2/1.9	No/Yes/Yes	≈0.0/3.1/1.6	No/Yes/Yes	0.4/3.4/1.7	No/Yes/Yes
ΔE_{ZPE} [kJ mol^{-1}][f]	0		0.1		0.7		0.8	
N[g]		506		233		232		262
σ [kHz][h]		14		14		15		14

[a] A, B, and C are the rotational constants. [b] D_J, D_{JK} and D_K are centrifugal distortion constants. [c] χ_{aa}, χ_{bb}, and χ_{cc} are the ^{14}N quadrupole coupling constants. [d] P_{aa}, P_{bb} and P_{cc} are the planar moments of inertia. [e] μ_a, μ_b and μ_c are the dipole moments at each inertial axis. [f] ΔE_{ZPE}, is the relative energy difference to the lowest energy conformers. [g] Number of fitted transitions. [h] Root-mean-square deviation of the fit. [i] Error is given in parentheses in units of the last digit.

considering an energy window up to 20 kJ mol^{-1}, predicted eight stable conformations. Four of them were absent in the conformational search and added to the list of potential conformers. The highest considered relative energy conformation is 4.2 kJ mol^{-1} above the global minimum (Fig. 2 and Tables S1 and S2, ESI†).

The conformers differ in the orientation of the carbonyl and two ethyl chains. Thus, there are three dihedral angles which define each conformer. The first dihedral, δ (C6–C1–C8–O1), atom labelling in Fig. 1, indicates the position of the carbonyl relative to the toluene. This dihedral can adopt four values of around ±50° (±*sc*) or around ±120° (±*ac*). The other two dihedrals, ϕ (C8–N1–C9–C11) and θ (C8–N1–C10–C12), define the relative orientation of the two *N*-ethyl chains located in *cis* and *trans* position of amide group respectively. Both can adopt two dispositions, with the angle being either positive or negative and values near ±80 (± *sc*) for the dihedral angle ϕ and ±120° (± *ac*) for the dihedral angle θ. The combination of the four dispositions of δ and two dispositions for ϕ and θ dihedral angles results in a total of eight enantiomeric pairs of conformations for DEET (Fig. 2, S1, and S2, ESI†). Since the enantiomers have the same rotational spectrum, we don't distinguish between them in the remainder of the paper for conciseness. The conformers are named by the three dihedral angles δ, ϕ, and θ followed by the relative energy ordering, with 1 being the most stable one. Thus, the lowest energy structure of DEET corresponds to +*sc*/−*ac*/−*sc* 1, while the highest energy isomer considered here would be +*ac*/−*ac*/+*sc* 8 (Fig. 2).

It is interesting that the conformers group in four pairs of almost iso-energetic structures. The conformers of each pair have similar values of the rotational constants, dipole moment components, and they exhibit opposed configurations for both amid-ethyl chains (Fig. 2). From the total of eight conformers, the four ones lowest in energy have been observed in the experimental spectrum, while the other four are missing. This could be due to relaxation processes of the higher energy forms into the lower energy structures by collisions at the initial stages of the supersonic expansion. To explore this, we performed scans for each dihedral angle, keeping the other two dihedrals fixed. Each DEET conformer is connected to three other conformers by the change in just one angle, thus one-dimensional scans are enough to investigate the connections between eight forms (Fig. S2, ESI†). A similar behaviour was recently observed in another molecule studied by microwave spectroscopy, alpha-methoxy phenylacetic acid.[26] The connections of the DEET conformers are summarized in Fig. S2 (ESI†). The relaxed scans are represented in Fig. S3–S5 (ESI†) for the change of each of the dihedral angles. The analysis of the energy barriers for the potential energy surfaces shows that four higher-energy conformers relax to the four energetically low-lying structures due to the essentially barrier-free torsion about the δ dihedral angle, indicating that they might not be real minima (Fig. S3, ESI†), thereby explaining why the initial conformational search failed to find these conformers. The other two torsions connecting conformers upon changing the ϕ and θ dihedrals are obstructed by a rather high energy barrier (Fig. S4 and S5, ESI†). Thus, the most possible explanation for the absence of those conformers is that +*sc*/+*ac*/+*sc* 5 relaxes into +*ac*/+*ac*/+*sc* 2; +*ac*/−*ac*/+*sc* 8 into +*sc*/−*ac*/+*sc* 3; +*sc*/+*ac*/−*sc* 7 into +*ac*/+*ac*/−*sc* 4; and finally +*ac*/−*ac*/−*sc* 6 into +*sc*/−*ac*/−*sc* 1 (Fig. S2, ESI†). Conversely, the barriers hindering the interconversion between the observed species are much higher than the 4.8 kJ mol^{-1} limit estimated for a relaxation in a Ne supersonic expansion.[27,28]

Microwave spectrum

A highly dense broadband spectrum was observed (Fig. S6, ESI†). The lines show the characteristic pattern of μ_b-type R-branch transitions (Fig. 3). Four sets of rotational constants could be obtained from spectral analysis and assigned to the

lower-energy four out of eight predicted conformations of DEET. The task was completed by comparing the agreement of the rotational constants, planar moments of inertia, nuclear quadrupole coupling constants, and dipole moment components with the theoretical values (Table 1). The spectra were assigned using a semirigid rotor Hamiltonian in the symmetric reduction and the I^r representation.[8] A comprehensive list of measured transitions is collected in Tables S3–S6 (ESI†).

Examining the parameters in Table 1, the assignment is straightforward as they are grouped in pairs based on the corresponding angles (δ and ϕ). The first pair, comprised by conformers *+sc/−ac/−sc* 1 and *+sc/−ac/+sc* 3 features close values of the rotational constants B and C, with A differing more, but similar enough to be paired together. Some correspondence can also be seen in the planar moments of inertia (Table 1). The presence of a nitrogen atom in the molecule induces a hyperfine structure due to the nuclear quadrupole coupling, which we were able to resolve (Fig. S7, ESI†) and obtain a set of nuclear quadrupole coupling constants. Those are in a good agreement with the theoretical predictions (Table 1). Although, the final corroboration that those two conformers belong to the same group is given by the dipole moment components (Table 1). Both structures, *+sc/−ac/−sc* 1 and *+sc/−ac/+sc* 3 have a low electric dipole moment μ_a and a large component μ_b. The dihedral angle δ, which defines the orientation of the amide, is approximately 52° for both *+sc/−ac/−sc* 1 and *+sc/−ac/+sc* 3. The two conformers can be distinguished by the dihedral θ, being −82° for *+sc/−ac/−sc* 1, while being 80° for *+sc/−ac/+sc* 3.

The second pair comprises conformers *+ac/+ac/+sc* 2 and *+ac/+ac/−sc* 4. As in the previous case, both species have similar rotational constants and planar moments of inertia (Table 1). For this family the dihedral angle δ is around 120°. The *+ac/+ac/+sc* 2 conformer dihedral θ is at 82°, while being −80° for conformer *+ac/+ac/−sc* 4. The two lowest energy conformers, *+sc/−ac/−sc* 1 and *+ac/+ac/+sc* 2, are characterized by the opposed configurations of ethyl chains. Both structures are isoenergetic and more stable than their counterparts, *+sc/−ac/+sc* 3 and *+ac/+ac/−sc* 4, so it is reasonable to argue that the most important contribution to the stability of the structures in DEET is the orientation of the amide-ethyl chains.

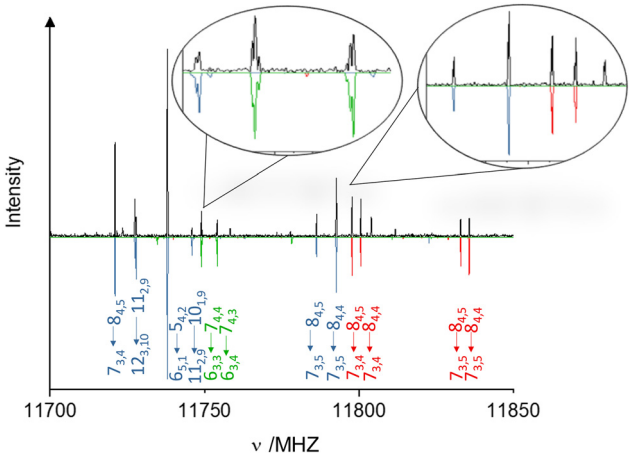

Fig. 3 Excerpt of the DEET spectrum. The observed experimental spectrum is shown in the upward-pointing black trace, and the fitted spectra are displayed in the downward-pointing coloured trace. Selected rotational transitions are shown for *+sc/−ac/−sc* 1 (red), *+ac/+ac/+sc* 2 (blue), and *+ac/+ac/−sc* 4 (green) where the hyperfine structure can be observed. The full recorded spectrum is given in Fig. S6 (ESI†).

Relative populations

The relative populations of the conformers in the supersonic jet can be estimated from the experimental transition intensities of the spectrum. Those intensities are assumed to be proportional to $N_i \cdot \mu_{i,\alpha}^2$, N_i being the number density of i species in the supersonic jet, and $\mu_{i,\alpha}$ the corresponding electric dipole moment component for the transition. Considering all the observed rotational transitions (Tables S3–S6, ESI†) the relative populations ratio is (in the same sequence as in Table 1) 34.4(0.8)/34.4(0.7)/17.2(0.6)/13.9(0.5), errors in parenthesis. As expected, conformers *+sc/−ac/−sc* 1 and *+ac/+ac/+sc* 2 have almost the same abundance in the supersonic expansion and are more populated that the *+sc/−ac/+sc* 3 and *+ac/+ac/−sc* 4 species which also have the same abundance as each other. The relative populations can also be estimated from the theoretical calculations considering the Gibbs free energies at the experimental conditions. In this case, as the eight conformations are close in energy, we expect a relatively even distribution of the theoretical populations. However, it is important to consider the relaxation pathways described for the higher energy conformers. Thus, their theoretical populations will be added to those of the conformers into which they relax. The relative populations calculated for the eight conformers at 423 K are, in the same order than in Fig. 2, from top to bottom and from left to right, 23.3/6.7/13.6/4.4/39.0/9.1/2.2/1.7 respectively at the B3LYP-D3BJ/def2-TZVP level of theory (Table S2, ESI†). Adding the populations of the non-observed conformers to those into which they relax results in a relative population of 32.3/45.7/15.3/6.6, in good agreement with the experimental populations (Table S2, ESI†). Surprisingly, even though the level of theory is the same (B3LYP-D3BJ/def2-TZVP), the populations using the Gibbs free energies from the Orca computations are in much better agreement with the experimental values than those from Gaussian.

Internal rotation

DEET has a methyl top bound to the benzyl ring, which can rotate with respect to the molecular frame. The internal rotation causes each transition to exhibit a fine structure (fs) resulting from the interaction of the internal and overall rotation. The lines appear as doublets of A and E torsional symmetry species, and the distance between both components depends on the height of the potential barrier (V_3) hindering internal rotation.[8] The internal rotation of toluene-like molecules has been studied.[29,30] These molecules are characterized by very low values for the internal rotation barrier, V_3, which makes the spectroscopic analysis challenging. An energy scan for the three methyl groups of DEET was performed to predict

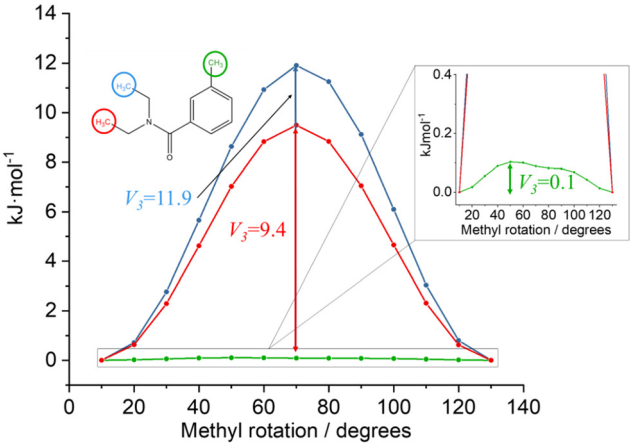

Fig. 4 Internal rotation barrier scans at B3LYP-D3BJ/def2TZVP level of theory with 12 steps of 10° size for the three methyl tops in DEET in the +*sc*/−*ac*/−*sc* 1 conformer. The scans for the other conformers are similar.

the barrier height value (Fig. 4). As expected, the alkyl chain's methyl groups have barriers of 11.9 kJ mol^{-1} and 9.4 kJ mol^{-1}, respectively. These values are high enough to exclude them from causing a fs. However, the methyl top attached to the benzene ring has a predicted barrier of around 0.1 kJ mol^{-1} (8.6 cm^{-1}). This value is similar to other toluene-like molecules and is characteristic of an almost free rotor. The low value of the internal rotation barrier causes a fs that can span several GHz in the spectrum, making it challenging to identify the *E* component. This work does not include an analysis of the internal rotation barrier of DEET, and only the *A* state transitions were included in the fits.

Intramolecular interactions

The relative stability of the four measured DEET conformers can be interpreted using non-covalent interaction (NCI) plots[31,32] to study intramolecular interactions. Such NCI plots (Fig. 5) help to visualize and characterize the attractive or repulsive forces. The Laplacian of the electron density, $\nabla^2\rho$, is a commonly used tool to distinguish between different interaction types. The Laplacian of the electron density Hessian matrix has contributions from all three principal axes of maximal variation, each with its own eigenvalue. The second eigenvalue, λ_2, distinguishes between various types of non-covalent interactions, including hydrogen bonding, dispersion, and steric interactions. A negative λ_2 indicates strong attraction, while a positive λ_2 implies repulsive interactions. Values close to 0 are typically interpreted as weak interactions.

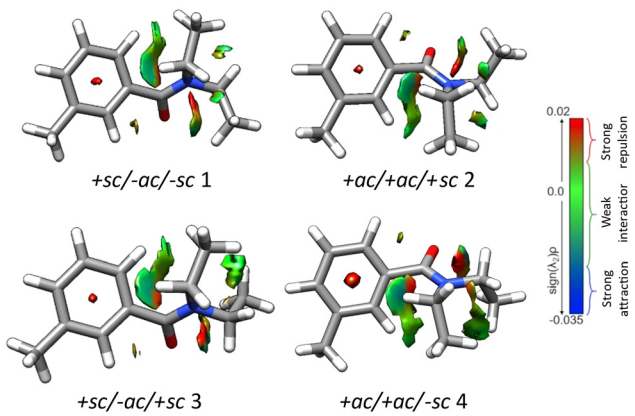

Fig. 5 Non-covalent interaction (NCI) analysis for the four detected DEET conformers; the sign of λ_2 distinguishes the different types of interactions.

In the case of DEET, the four isomers exhibit similar interactions. The conformers are stabilized by a CH···π attraction from one of the ethyl groups to the benzene ring. The other ethyl group establishes a CH···O interaction with the carbonyl (Fig. 5). Beside those interactions, the conformers in +*sc*/−*ac*/+*sc* 3 and +*ac*/+*ac*/−*sc* 4 present a more dominant CH···HC interaction between the two ethyl groups (Fig. 5). In the four cases, there is another common attraction located between the oxygen and one of the aromatic ring hydrogen atoms. The difference in the stability between the +*sc*/−*ac*/−*sc* 1 – +*ac*/+ *ac*/+*sc* 2 and +*sc*/−*ac*/+*sc* 3 – +*ac*/+*ac*/−*sc* 4 conformations could be explained in terms of the force present in the amide region, which seems to be less attractive and more repulsive for conformers +*sc*/−*ac*/+*sc* 3 and +*ac*/+*ac*/−*sc* 4 (Fig. 5).

Conclusions

We explored the structure and intramolecular interactions of the most used synthetic repellent, DEET. The current work reinforces the use of rotational spectroscopy assisted by computational modelling as a powerful tool for accurate conformational analysis of flexible biomolecules. A careful analysis of the experimental rotational spectrum has detected four conformers, predicted to have rather low relative energies according to theoretical computations. We also estimated the relative populations from the experimental intensities, corroborating their closeness to the theoretical predictions. DEET exhibits a methyl top, behaving as an almost-free rotor, similar to the methyl group in toluene. This work provides the foundations for future microsolvation and molecular recognition studies of intermolecular complexes to elucidate the structure–activity relationship of these types of compounds.

Author contributions

Otger Crehuet: conceptualization, investigation, formal analysis, writing – first draft, writing – review and editing. Andrea Vázquez: formal analysis, writing – review and editing. Pablo Pinacho: formal analysis, writing – review and editing. Aran Insausti: investigation, formal analysis, writing – review and editing. Elena R. Alonso: formal analysis, writing – review and editing. Francisco J. Basterretxea: funding acquisition, project administration, writing – review and editing. Emilio J. Cocinero: conceptualization, funding acquisition, project administration, writing – review and editing.

Data availability

The data supporting this article have been included as part of the ESI.†

Conflicts of interest

The authors declare no conflicts of interest.

Acknowledgements

Financial support from the MINECO (PID2020-117892RB-I00), Basque Government (IT1491-22, IT1162-19 and PIBA 2018-11), the UPV/EHU (PPG17/10 and GIU18/207) is acknowledged. P. P. acknowledges a Maria Zambrano grant (UPV/EHU, Ministry of Universities, Recovery, Transformation, and Resilience Plan – Funded by the European Union – Next Generation EU, MAZAM22/16). E. R. A. acknowledges Juan de la Cierva grant (FJC2018-037320-I) of the Ministerio de Ciencia e Innovación. The laser and computational resources of the UPV/EHU (SGIker) were used.

References

1 E. T. McCabe, W. F. Barthel, S. I. Gertler and S. A. Hall, *J. Org. Chem.*, 1954, **19**, 493–498.
2 S. J. Moore and M. Debboun, in *Strickman, Insect repellents: principles, methods, and uses*, ed. M. Debboun, S. P. Frances, CRC Press, 2007, Boca Raton.
3 T. M. Katz, J. H. Miller and A. A. Hebert, *J. Am. Acad. Dermatol.*, 2008, **58**, 865.
4 J. D. Bohbot and J. C. Dickens, *PLoS One*, 2010, **5**, e12138.
5 M. Ditzen, M. Pellegrino and L. B. Vosshall, *Science*, 2008, **319**, 1838–1842.
6 E. B. Dogan, J. W. Ayres and P. A. Rossignol, *Med. Vet. Entomol.*, 1999, **13**, 97–100.
7 Z. Syed and W. S. Leal, *Proc. Natl. Acad. Sci. U. S. A.*, 2008, **105**, 13598–13603.
8 W. Gordy and R. L. Cook, *Microwave Molecular Spectra*, Wiley, 1984, New York.
9 L. B. Favero, I. Uriarte, L. Spada, P. Écija, C. Calabrese, W. Caminati and E. J. Cocinero, *J. Phys. Chem. Lett.*, 2016, **7**, 1187–1191.
10 S. R. Domingos, C. Pérez, C. Medcraft, P. Pinacho and M. Schnell, *Phys. Chem. Chem. Phys.*, 2016, **18**, 16682–16689.
11 D. Banser, M. Schnell, J. U. Grabow, E. J. Cocinero, A. Lesarri and J. L. Alonso, *Angew. Chem.*, 2005, **44**, 6311–6315.
12 V. A. Shubert, D. Schmitz and M. Schnell, *J. Mol. Spectrosc.*, 2014, **300**, 31–36.
13 D. Patterson, M. Schnell and J. Doyle, *Nature*, 2013, **497**, 475–477.
14 I. Uriarte, C. Pérez, E. Caballero-Mancebo, F. J. Basterretxea, A. Lesarri, J. A. Fernández and E. Cocinero, *Chem. – Eur. J.*, 2017, **23**, 7238–7244.
15 I. Uriarte, P. Écija, L. Spada, E. Zabalza, A. Lesarri, F. J. Basterretxea, J. A. Fernández, W. Caminati and E. J. Cocinero, *Phys. Chem. Chem. Phys.*, 2016, **18**, 3966–3974.
16 A. Insausti, E. R. Alonso, B. Tercero, J. I. Santos, C. Calabrese, N. Vogt, F. Corzana, J. Demaison, J. Cernicharo and E. J. Cocinero, *J. Phys. Chem. Lett.*, 2021, **12**(4), 1352–1359.
17 C. Calabrese, I. Uriarte, A. Insausti, M. Vallejo-López, F. J. Basterretxea, S. A. Cochrane, B. G. Davis, F. Corzana and E. J. Cocinero, *ACS Cent. Sci.*, 2020, **6**, 293–303.
18 F. Mohamadi, N. G. J. Richards, W. C. Guida, R. Liskamp, M. Lipton, C. Caufield, G. Chang, T. Hendrickson and W. C. Still, *J. Comput. Chem.*, 1990, **11**, 440–467.
19 T. A. Halgren, *J. Comput. Chem.*, 1996, **17**, 553–586.
20 A. D. Becke, *J. Chem. Phys.*, 1993, **98**, 5648–5652.
21 C. Lee, W. Yang and G. R. Parr, *Phys. Rev. B: Condens. Matter Mater. Phys.*, 1988, **37**, 785–789.
22 S. Grimme, J. Antony, S. Ehrlich and H. Krieg, *J. Chem. Phys.*, 2010, **132**, 154101.
23 M. J. Frisch, G. W. Trucks, H. B. Schlegel, G. E. Scuseria, M. A. Robb, J. R. Cheeseman, G. Scalmani, V. Barone, G. A. Petersson, H. Nakatsuji, X. Li, M. Caricato, A. V. Marenich, J. Bloino, B. G. Janesko, R. Gomperts, B. Mennucci, H. P. Hratchian, J. V. Ortiz, A. F. Izmaylov, J. L. Sonnenberg, D. Williams-Young, F. Ding, F. Lipparini, F. Egidi, J. Goings, B. Peng, A. Petrone, T. Henderson, D. Ranasinghe, V. G. Zakrzewski, J. Gao, N. Rega, G. Zheng, W. Liang, M. Hada, M. Ehara, K. Toyota, R. Fukuda, J. Hasegawa, M. Ishida, T. Nakajima, Y. Honda, O. Kitao, H. Nakai, T. Vreven, K. Throssell, J. A. Montgomery Jr., J. E. Peralta, F. Ogliaro, M. J. Bearpark, J. J. Heyd, E. N. Brothers, K. N. Kudin, V. N. Staroverov, T. A. Keith, R. Kobayashi, J. Normand, K. Raghavachari, A. P. Rendell, J. C. Burant, S. S. Iyengar, J. Tomasi, M. Cossi, J. M. Millam, M. Klene, C. Adamo, R. Cammi, J. W. Ochterski, R. L. Martin, K. Morokuma, O. Farkas, J. B. Foresman and D. J. Fox, *Gaussian 16, Revision A.03*, Gaussian, Inc., Wallingford CT, 2016.
24 (*a*) F. Neese, *Wiley Interdiscip. Rev.: Comput. Mol. Sci.*, 2012, **2**, 73–78; (*b*) F. Neese, *Wiley Interdiscip. Rev.: Comput. Mol. Sci.*, 2022, **12**, e1606.
25 G. G. Brown, B. C. Dian, K. O. Douglass, S. M. Geyer, S. T. Shipman and B. H. Pate, *Rev. Sci. Instrum.*, 2008, **79**, 053103.
26 H. Singh, P. Pinacho, D. A. Obenchain, M. M. Quesada-Moreno and M. Schnell, *Phys. Chem. Chem. Phys.*, 2022, **24**, 27312–27320.
27 R. S. Ruoff, T. D. Klots, T. Emilsson and H. S. Gutowsky, *J. Chem. Phys.*, 1990, **93**, 3142–3150.
28 P. Pinacho, J. C. López, Z. Kisiel and S. Blanco, *Phys. Chem. Chem. Phys.*, 2020, **22**, 18351–18360.
29 D. A. Obenchain, P. Pinacho, S. Zinn and M. Schnell, *J. Mol. Struct.*, 2020, **1213**, 128109.
30 K. P. Rajappan Nair, S. Herbers and J. U. Grabow, *J. Mol. Spectrosc.*, 2019, **355**, 19–25.
31 E. R. Johnson, S. Keinan, P. Mori-Sánchez, J. Contreras García, A. J. Cohen and W. Yang, *J. Am. Chem. Soc.*, 2010, **132**, 6498–6506.
32 J. Contreras-García, E. R. Johnson, S. Keinan, R. Chaudret, J. P. Piquemal, D. N. Beratan and W. Yang, *J. Chem. Theory Comput.*, 2011, **7**, 625–632.

